

Command-Filter-Based Finite-Time Fault-Tolerant Control of Attitude Tracking for Quadrotor UAVs with Actuator Faults

Boning Li, Ming Chen, Shuchang Qi

Abstract—A finite-time controller of attitude tracking is designed for quadrotor unmanned aerial vehicles (UAVs). In order to avoid the differential explosion problem existing in the traditional backstepping method, a command filter is introduced. In addition, as for the possible actuator faults, fault-tolerant control is incorporated into the controller, in which the parameter estimators are designed to identify the unknown fault parameters in the system. Through the comprehensive application of finite-time control, adaptive control and fault-tolerant control, the proposed controller ensures that the system's rapidity, robustness and reliability are improved. Finally, the validity and stability of our present control scheme are verified by a numerical simulation.

Index Terms—quadrotor UAV, finite-time, command filtering, fault-tolerant control.

I. INTRODUCTION

During the Second World War, quadrotor UAVs were manufactured and used to carry out some dangerous reconnaissance missions, invade strategic locations and other military tasks, wherein they demonstrated their strong mobility and flexibility, and played an important role in the acquisition of war intelligence. The performance of the quadrotor UAVs are superior; that is, they have the advantages of good performance, small size, many functions, and sensitive actions. Especially in recent years, with the continuous development of control technology, the quadrotor UAVs have been widely used in various fields such as aerospace, geological surveys, agricultural surveys, and danger rescue. Generally speaking, the control tasks of quadrotor UAVs mainly include attitude control, trajectory tracking, positioning, and navigation. Among them, the attitude tracking control of the quadrotor UAVs is one of the important subjects which has attracted extensive attention of many scholars at home and abroad. However, since the attitude control systems of UAVs are multi-variable, nonlinear and strongly coupled, it is a challenging task to maintain the stability of the attitude systems [1], [2]. As a result, it is very important theoretical and

practical value to study the problem of attitude control of UAVs by using advanced control theories and methods.

Up to now, a variety of algorithms, such as PID (Proportional Integral Differential)[3], [4], SMC (sliding mode control)[5]–[7], backstepping scheme[8]–[10], and adaptive control[11], have been applied to the attitude control of quadrotor UAVs and achieved good control effect. It is discovered that the backstepping is one of the most widely used and typical methods. In [4], attitude tracking control was achieved using a class of saturated proportional-derivative (PD) control laws. In [11], a new backstepping sliding mode controller is constructed for the attitude tracking of UAVs with external disturbances. In [12], a backstepping strategy is applied to a quadrotor UAV. In [13], an auxiliary system for dealing with an input saturation problem was constructed. Traditional control scheme do not deal well with actuator failures. Therefore, it is urgent to design some more suitable controllers with the combination of backstepping and other advanced theories for controlling the attitude of UAVs. Through the literature review, it was found that backstepping adaptive methods have attracted considerable attention. In order to improve the robustness and the tracking performance of the nonlinear UAV quadrotor system, an adaptive backstepping sliding mode approach, was presented in [9]. Nevertheless, in backstepping control, the derivatives of the virtual control law need to be calculated which inevitably increased computational pressure. In addition, the model of a quadrotor UAV system itself is very complex. This complicates the calculation problem. Based on the above analysis, in this paper, we intend to introduce a command filter to solve the complex calculation problem so as to make the designed controller easier to implement.

On the other hand, a quadrotor UAV system is generally composed of many components and has a complex structure. Obviously, in the course of its operation, any component inevitably failed. Among them, as the most critical components, the consequences are unimaginable once actuators fail. So it is of great significance to design some controllers that can ensure the normal operation in the event of some actuator failures. In [14], an actuator fault detection method is proposed for a quadrotor UAV based on the linear-parameter-varying (LPV) model which enhances the fault sensitivity. In [15], the authors present an active fault tolerant control strategy for a quadrotor UAV with actuator failure. In [16], the issues of the propeller damage and actuator fault are considered simultaneously, and the passive and active fault-tolerant controllers are designed. However, the implementation of the above controllers are based on the assumption that velocity information is available. As

Manuscript received April 8, 2024; revised September 8, 2024. This work was supported by the National Natural Science Foundation of China under Grant U21A20483, 61873024 and 61773072.

Boning Li is a postgraduate student in the Department of Electronic Information, University of Science and Technology Liaoning, 114051, China. (phone: 13614132315, fax: 0412-5929093, e-mail 1104832500@qq.com)

Ming Chen is a professor in the Department of Electronic Information, University of Science and Technology Liaoning, Anshan, Liaoning, 114051, China.(phone: 13609800566, fax: 0412-5929093, e-mail: cm8061@sina.com)

Shuchang Qi is a postgraduate student in the Department of Electronic Information, University of Science and Technology Liaoning, Anshan, Liaoning, 114051, China. (phone: 15566271068, fax: 0412-5929093, e-mail: 13898153982@163.com)

for the unavailable information, the neural network-based fault-tolerant control scheme is proposed to compensate for parametric uncertainties, external disturbances and actuator faults. Although the problem of the quadrotor UAV system actuator fault has been resolved somewhat, the estimation of the above fault parameters is only the estimation of the parameters. Our presented method can effectively solve this problem, in other words, we try to achieve a good control effect by only estimating bounds of actuator fault parameters.

In addition, it is one of the important control objectives to improve the tracking speed in the process of attitude tracking of quadrotor UAVs. Fortunately, finite-time control provides the theoretical support for realizing this goal. Compared with infinite-time control, the advantage of finite-time control is that it has strong tracking performance and anti-interference performance and can achieve the better transient performance of the systems. In [17], [18], two different finite-time sliding mode controllers are designed for quadrotor UAVs. And the simulation results show that the system states are forced to converge to the synovial planes in finite time. In this paper, finite-time control will be introduced into our design framework, that is, it is combined with backstepping, command filtering and adaptive control, in order to improve the tracking speed of the UAV.

Based on the above literature review, it can be concluded that the combination of the backstepping and other advanced theories and methods can achieves better control. for attitude tracking in quadrotor UAVs. In our design, the key issues include: reduction of the convergence time, improvement of the system reliability, relative stability and control accuracy. In particular, inspired by [19], wherein a finite-time adaptive tracking problem is investigated for nonlinear systems with unknown control gain functions and actuator failures, the attitude control problem of a quadrotor UAV with actuator failure is considered. Specifically, under the condition of considering the actuator failures, for the first time, the backstepping, finite-time control, adaptive, and command filtering technologies were combined to realize UAV attitude controller design. Compare with the existing results, our proposed controller has the following advantages:

- (i) The attitude controller in this paper has smaller attitude angle tracking error and shorter convergence time.
- (ii) A first-order low-pass filter and a compensation mechanism is introduced to avoid the problem of complex matrix derivation, and effectively reduce the complexity of the controller structure.
- (iii) The designed controller can handle any fault in a given range and has strong robustness.

The remainder of this paper is organized as follows. In the second part, we describe the model of a quadrotor UAV, and provide some necessary inequalities needed for the controller design in the following section. Next, the controller is designed and its stability is analyzed. In the fourth part, we verify the effectiveness and feasibility of the proposed method through simulation experiments. At last, the full paper is summarized and the future work is prospected.

II. MODEL DESCRIPTION AND PREPARATORY KNOWLEDGE

A. Model of quadrotor UAV

In this section, a quadrotor UAV system model is considered as Figure 1 in which two coordinate systems are established. One is the earth coordinate system with the earth as the reference. In this system, b_1 -axis points east, and the b_2 -axis, b_3 -axis point north and skyward, respectively. The other is the inertial coordinate system with the quadrotor UAV as the reference. In this system, c_1 -axis points right, and c_2 -axis, c_3 -axis forward and above, respectively. No matter how the position of the quadrotor UAV changes, the inertial coordinate system is the same all the time. ϕ , θ and ψ represent roll, pitch, yaw, respectively. Four rotors are driven by four motors represented by $M_i (i = 1, 2, 3, 4)$. Among them, M_2, M_4 drive the rotor to rotate clockwise; and M_1, M_3 drive the rotor to rotate counterclockwise. We design the controller to make sure that ϕ , θ and ψ quickly track their reference signals.

Before introducing the attitude control model, some assumptions are needed.

Assumption 1 The effect of drag and propeller dynamics on the UAV is ignored.

Assumption 2 The structural parameters of the UAV itself remain unchanged.

Assumption 3 The expected signals and their time derivatives are bounded.

Next, a quadrotor UAV attitude dynamics model is provided, which is established as

$$\begin{cases} \dot{\Theta} = \mathbf{R}(\Theta)\omega \\ \mathbf{J}\dot{\omega} = -\omega \times \mathbf{J}\omega + \tau \\ y = \Theta \end{cases} \quad (1)$$

where $\Theta = [\phi, \theta, \psi]^T$ is the Euler Angle, and $\tau \in \mathbf{R}^3$ and $y \in \mathbf{R}^3$ represent input the output, respectively. And $\tau = [\tau_1, \tau_2, \tau_3]^T$, $\tau_i, i = 1, 2, 3$, is the torque component of each axe. $\mathbf{R}(\cdot)$ represents the nonsingular rotation matrix, which can achieve the transformation from the angular velocity ω to the Euler Angle change rate $\dot{\Theta}$, and $\mathbf{R}(\cdot)$ is represented as

$$\mathbf{R}(\Theta) = \begin{bmatrix} 1 & s_\phi t_\theta & c_\phi t_\theta \\ 0 & c_\phi & -s_\phi \\ 0 & s_\phi/c_\theta & c_\phi/c_\theta \end{bmatrix} \quad (2)$$

where $s_\phi = \sin \phi$, $t_\theta = \tan \theta$, $c_\phi = \cos \phi$, $c_\theta = \cos \theta$. The physical input of the quadrotor UAV is a PWM(Pulse Width Modulation) signal sent to the ESC (Electronic Speed Controller), and the following transformation relationship holds.

$$\begin{bmatrix} u \\ \tau_1 \\ \tau_2 \\ \tau_3 \end{bmatrix} = \begin{bmatrix} k_u & k_u & k_u & k_u \\ -k_u r_1 & k_u r_1 & k_u r_1 & -k_u r_1 \\ k_u r_2 & k_u r_2 & -k_u r_2 & -k_u r_2 \\ K_\tau & -K_\tau & K_\tau & -K_\tau \end{bmatrix} \begin{bmatrix} W_1^2 \\ W_2^2 \\ W_3^2 \\ W_4^2 \end{bmatrix} \quad (3)$$

where u represents the total thrust produced by all the propellers. k_u stands for the torque, and k_τ denotes the inverse torque constant. r_1, r_2 represent the arm length. The speed of the four motors is represented by $W_i^2 (i = 1, 2, 3, 4)$.

Inspired by [20], (1) is assumed subject to actuator faults, and the fault model is described as

$$\tau^F = \rho\tau + \sigma \quad (4)$$

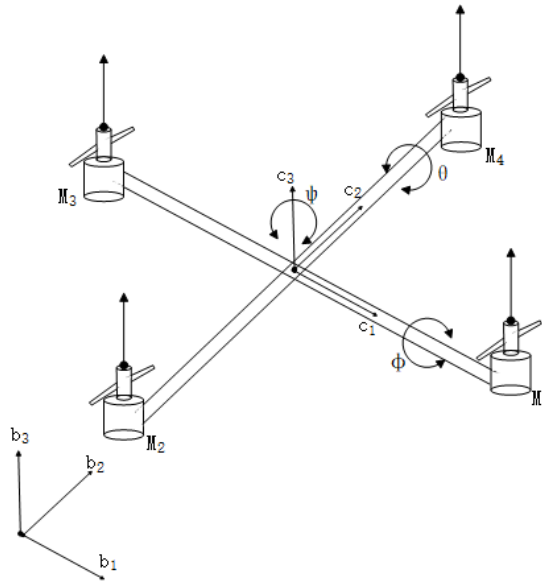


Fig. 1. Structural diagram of a quadrotor UAV.

where $\tau^F = [\tau_1^F, \tau_2^F, \tau_3^F]^T$, $\sigma = [\sigma_1, \sigma_2, \sigma_3]^T$, $\rho = \text{diag}(\rho_1, \rho_2, \rho_3)$, $\rho_i \in (0, 1]$ $i = 1, 2, 3$. σ_1, σ_2 and σ_3 are bounded.

(1) $\rho = \text{diag}(1, 1, 1)$, $\sigma = [0, 0, 0]^T$. The fault-free case.

(2) $0 < \rho_i < 1$, $\sigma_i \neq 0$, $i = 1, 2, 3$. The partial loss of effectiveness fault.

The control objective of this article is to design a controller to drive the actual output y of the quadrotor UAV to track a reference signal in finite-time in the event of the actuator failures.

B. Preparatory knowledge

Lemma 1[21] For a given constant $\epsilon > 0$ and $x \in R$, the following inequality is true.

$$0 \leq |x| - x \tanh\left(\frac{x}{\epsilon}\right) \leq 0.2785\epsilon \quad (5)$$

Lemma 2[22] For any given positive numbers a_1, a_2, a_3 , the following inequality holds.

$$\begin{aligned} |x|^{a_1} |y|^{a_2} &\leq \frac{a_1}{a_1 + a_2} a_3 |x|^{a_1 + a_2} \\ &+ \frac{a_2}{a_1 + a_2} a_3^{\frac{a_1}{a_2}} |y|^{a_1 + a_2} \end{aligned} \quad (6)$$

where $x, y \in R$.

Lemma 3[23] Consider a nonlinear system $\dot{x}(t) = f(x(t))$. If there exists a function $V(x)$ such that

$$\dot{V}(x) \leq -\varrho V(x) - \varkappa V^p(x) + h \quad (7)$$

where $\varrho > 0$, $\varkappa > 0$, $h > 0$, $0 < p < 1$, then the nonlinear system is finite-time stable. And the settling time is

$$t \leq T_c = \frac{1}{\varrho(1-p)} \ln \frac{\varrho V^{1-p} + \lambda \varkappa}{\lambda \varkappa} \quad (8)$$

where $\lambda \in (0, 1)$.

Lemma 4[24] For $x_i \in R, i = 1, 2, \dots, n$, and $p \in (0, 1)$, the following inequality holds.

$$(x_1 + \dots + x_n)^p \leq |x_1|^p + \dots + |x_n|^p \quad (9)$$

III. CONTROLLER DESIGN

In this section, a new control scheme based on the backstepping method is proposed for the attitude model of the UAV with actuator faults. The design process of the controller has the following two steps

Step 1.

Following the general design rules of the backstepping method, The following coordinate transformations are introduced as

$$\mathbf{z}_1 = \Theta - \Theta_d \quad (10)$$

$$\mathbf{z}_2 = \omega - \bar{\alpha} \quad (11)$$

where $\Theta_d = [\phi_d, \theta_d, \psi_d]^T$ is a reference signal. $\bar{\alpha} \in R^{3 \times 1}$ is a filtered output, and the filter is given as

$$\varepsilon \bar{\alpha}' + \bar{\alpha} = \alpha \quad (12)$$

where $\varepsilon = \text{diag}(\varepsilon_1, \varepsilon_2, \varepsilon_3)$ represents a constant matrix to be designed. $\alpha \in R^{3 \times 1}$ is the input of the filter, and also represents the virtual control law in our controller design.

Remark 1 The backstepping method is used in the precess of controller design. To avoid taking the derivative of the virtual control law, the first-order low-pass filter is necessary.

In order to reduce or eliminate the effect of the filtering errors, the following compensating system is introduced

$$\dot{\xi}_1 = -k_1 \xi_1 + \mathbf{R} \bar{\alpha} - \mathbf{R} \alpha + \mathbf{R} \xi_2 - \mathbf{P} \mathbf{l}_1 \quad (13)$$

$$\dot{\xi}_2 = -k_2 \xi_2 - \mathbf{R} \xi_1 - \mathbf{Q} \mathbf{l}_2 \quad (14)$$

where $\xi_1 = [\xi_{11}, \xi_{12}, \xi_{13}]^T, \xi_2 = [\xi_{21}, \xi_{22}, \xi_{23}]^T, \mathbf{P} = \text{diag}(\text{sign}(\xi_{11}), \text{sign}(\xi_{12}), \text{sign}(\xi_{13})), \mathbf{Q} = \text{diag}(\text{sign}(\xi_{21}), \text{sign}(\xi_{22}), \text{sign}(\xi_{23})), k_1, k_2 \in (\frac{1}{2}, \infty), \mathbf{l}_1 = [l_{11}, l_{12}, l_{13}]^T$ and $\mathbf{l}_2 = [l_{21}, l_{22}, l_{23}]^T$ are parameter vectors to be designed.

By using (1) and (10), we have

$$\dot{\mathbf{z}}_1 = \mathbf{R}(\mathbf{z}_2 + \bar{\alpha}) - \dot{\Theta}_d \quad (15)$$

The compensated errors are defined as

$$\mathbf{e}_1 = \mathbf{z}_1 - \xi_1 \quad (16)$$

$$\mathbf{e}_2 = \mathbf{z}_2 - \xi_2 \quad (17)$$

With the help of (11) and (15), the derivative of (16) can be expressed as

$$\begin{aligned} \dot{\mathbf{e}}_1 &= \mathbf{R}(\mathbf{z}_2 + \bar{\alpha}_2) - \dot{\bar{\alpha}}_d + k_1 \xi_1 \\ &\quad - \mathbf{R}\bar{\alpha} + \mathbf{R}\alpha - \mathbf{R}\xi_2 + \mathbf{P}\mathbf{1}_1 \\ &= \mathbf{R}\mathbf{e}_2 - \dot{\bar{\alpha}}_d + \mathbf{R}\alpha + k_1 \xi_1 + \mathbf{P}\mathbf{1}_1 \end{aligned} \quad (18)$$

Consider a Lyapunov function V_1 as

$$V_1 = \frac{1}{2} \mathbf{e}_1^T \mathbf{e}_1 \quad (19)$$

Time differentiation of (19) gives

$$\dot{V}_1 = \mathbf{e}_1^T (\mathbf{R}\mathbf{e}_2 - \dot{\bar{\alpha}}_d + \mathbf{R}\alpha + k_1 \xi_1 + \mathbf{P}\mathbf{1}_1) \quad (20)$$

Now, the virtual control law is designed as

$$\alpha = \mathbf{R}^{-1}(-k_1 \mathbf{z}_1 + \dot{\bar{\alpha}}_d - c_1 (\mathbf{e}_1^T \mathbf{e}_1)^{\frac{2p-1}{2}}) \quad (21)$$

where c_1 positive, $0 < p < 1$.

From Lemma 4 and (21), we have

$$\begin{aligned} \dot{V}_1 &\leq -k_1 \mathbf{e}_1^T \mathbf{e}_1 + \mathbf{e}_1^T \mathbf{R}\mathbf{e}_2 - c_1 (\mathbf{e}_1^T \mathbf{e}_1)^p \\ &\quad + \mathbf{e}_1^T \mathbf{P}\mathbf{1}_1 \end{aligned} \quad (22)$$

From the property of the square inequality, the term $\mathbf{e}_1^T \mathbf{P}\mathbf{1}_1$ in (22) can be further derived

$$\mathbf{e}_1^T \mathbf{P}\mathbf{1}_1 \leq \frac{1}{2} \mathbf{e}_1^T \mathbf{e}_1 + \frac{1}{2} \|\mathbf{1}_1\|^2 \quad (23)$$

By bringing (23) into (22), we have

$$\begin{aligned} \dot{V}_1 &\leq -(k_1 - \frac{1}{2}) \mathbf{e}_1^T \mathbf{e}_1 - c_1 (\mathbf{e}_1^T \mathbf{e}_1)^p \\ &\quad + \mathbf{e}_1^T \mathbf{R}\mathbf{e}_2 + \frac{1}{2} \|\mathbf{1}_1\|^2 \end{aligned} \quad (24)$$

Step 2.

Based on (14), the time derivative of \mathbf{z}_2 is

$$\dot{\mathbf{z}}_2 = -\mathbf{J}^{-1}\omega \times \mathbf{J}\omega + \mathbf{J}^{-1}(\rho\tau + \sigma) + \mathbf{v} - \mathbf{v} - \bar{\alpha}' \quad (25)$$

Note that the intermediate control law $\mathbf{v} = [v_1, v_2, v_3]^T$ is introduced, and it is very necessary and plays a crucial role in our controller design.

In addition, the following parameters are needed to be defined.

$$s_i = \inf \rho_i \quad (26)$$

$$\beta_i = 1/s_i \quad (27)$$

$$\zeta_i = \sup s_i \quad (28)$$

where $i = 1, 2, 3$.

Next, we choose the following Lyapunov candidate function

$$V_2 = V_1 + \frac{1}{2} \mathbf{e}_2^T \mathbf{e}_2 + \sum_{i=1}^3 \left(\frac{s_i}{2\Gamma_i} \|\tilde{\beta}_i\|^2 + \frac{1}{2\gamma_i} \|\tilde{\zeta}_i\|^2 \right) \quad (29)$$

Define

$$\tilde{\beta}_i = \beta_i - \hat{\beta}_i \quad (30)$$

$$\tilde{\zeta}_i = \zeta_i - \hat{\zeta}_i \quad (31)$$

where $\Gamma_i, \gamma_i, i = 1, 2, 3$, are the positive number to be designed, and $\hat{\beta}_i, \hat{\zeta}_i$ are the estimated values of β_i and ζ_i .

The time derivative of V_2 is deduced

$$\begin{aligned} \dot{V}_2 &= \dot{V}_1 + \mathbf{e}_2^T [-\mathbf{J}^{-1}\omega \times \mathbf{J}\omega + \mathbf{J}^{-1}(\rho\tau + \sigma) + \mathbf{v} - \mathbf{v} - \bar{\alpha}' \\ &\quad + k_2 \xi_2 + \mathbf{R}\xi_1 + \mathbf{Q}\mathbf{1}_2] + \sum_{i=1}^3 \left(\frac{s_i}{\Gamma_i} \tilde{\beta}_i \tilde{\beta}_i' + \frac{1}{\gamma_i} \tilde{\zeta}_i \tilde{\zeta}_i' \right) \end{aligned} \quad (32)$$

We define

$$\mathbf{G} = [\hat{\zeta}_1 \tanh(\frac{\epsilon_{21}}{\epsilon_1}), \hat{\zeta}_2 \tanh(\frac{\epsilon_{22}}{\epsilon_2}), \hat{\zeta}_3 \tanh(\frac{\epsilon_{23}}{\epsilon_3})]^T \quad (33)$$

where $\epsilon_1, \epsilon_2, \epsilon_3$ are positive numbers.

Now, \mathbf{v} is designed as

$$\mathbf{v} = \mathbf{R}\mathbf{z}_1 + k_2 \mathbf{z}_2 + c_2 (\mathbf{e}_1^T \mathbf{e}_1)^{\frac{2p-1}{2}} + \mathbf{G} - \bar{\alpha}' - \mathbf{J}^{-1}\omega \times \mathbf{J}\omega \quad (34)$$

where $c_2 > 0$. Substituting (33)-(34) into (32), we have

$$\begin{aligned} \dot{V}_2 &\leq -(k_1 - \frac{1}{2}) \mathbf{e}_1^T \mathbf{e}_1 - (k_2 - \frac{1}{2}) \mathbf{e}_2^T \mathbf{e}_2 - c_1 (\mathbf{e}_1^T \mathbf{e}_1)^p \\ &\quad - c_2 (\mathbf{e}_2^T \mathbf{e}_2)^p + \frac{1}{2} \|\mathbf{1}_1\|^2 + \frac{1}{2} \|\mathbf{1}_2\|^2 + \mathbf{e}_2^T \mathbf{v} + \mathbf{e}_2^T \mathbf{J}^{-1} \rho\tau \\ &\quad + \sum_{i=1}^3 \left(\zeta_i (|e_{2i}| - e_{2i} \tanh(\frac{\epsilon_{2i}}{\epsilon_i})) + \frac{s_i}{\Gamma_i} \tilde{\beta}_i \tilde{\beta}_i' + \right. \\ &\quad \left. \frac{1}{\gamma_i} \tilde{\zeta}_i (\tilde{\zeta}_i' + r_i e_{2i} \tanh(\frac{\epsilon_{2i}}{\epsilon_i})) \right) \end{aligned} \quad (35)$$

The actual control input τ_i is designed as

$$\tau_i = - \frac{J_i e_{2i} \hat{\beta}_i^2 v_i^2}{\sqrt{e_{2i}^2 \hat{\beta}_i^2 v_i^2 + \varpi^2}} \quad (36)$$

where $\varpi > 0, J_1 = I_{xx}, J_2 = I_{yy}, J_3 = I_{zz}$.

At this point, the control law of the UAV is designed. If the lift F is known, the engine speed $W_i^2 (i = 1, 2, 3, 4)$ can be determined.

Further, the parameter adaptive laws are design as

$$\hat{\zeta}_i' = \gamma_i e_{2i} \tanh(\frac{\epsilon_{2i}}{\epsilon_i}) - n_1 \hat{\zeta}_i \quad (37)$$

$$\hat{\beta}_i' = \Gamma_i e_{2i} v_i - n_2 \hat{\beta}_i \quad (38)$$

where n_1, n_2 are the positive constants.

A. Analysis of stability

In this section, our conclusion is presented as follows.

Theorem 1 Consider the quadrotor system under Assumptions 1–3, the virtual control laws (21), the actual controller (36), and the adaptive updating laws (37) and (38) make sure that all the signals in the closed-loop system are bounded and the tracking errors converge to the residual sets, and the settling time can be computed as

$$T \leq \frac{1}{\varrho(1-p)} \ln \frac{\varrho V_2^{1-p} + \lambda \varkappa}{\lambda \varkappa} \quad (39)$$

where $\varrho = \min\{k - \frac{1}{2}\}, \varkappa = \min\{2^p, c_1, c_2, n_1, s_i n_2\}, 0 < p < 1, 0 < \lambda < 1, i = 1, 2, 3$.

Proof: From (36), one can obtain

$$\begin{aligned} e_{2i} J_i^{-1} \rho_i \tau_i &\leq -\rho_i \frac{e_{2i}^2 \hat{\beta}_i^2 v_i^2}{\sqrt{e_{2i}^2 \hat{\beta}_i^2 v_i^2 + \varpi^2}} \\ &\leq \frac{s e_{2i}^2 \hat{\beta}_i^2 v_i^2}{\sqrt{e_{2i}^2 \hat{\beta}_i^2 v_i^2 + \varpi^2}} \\ &\leq s_i n - s_i e_{2i} \hat{\beta}_i v_i \end{aligned} \quad (40)$$

According to Lemma 1, the following inequality holds

$$\zeta_i |e_{2i}| - e_{2i} \zeta \tanh\left(\frac{e_{2i}}{\epsilon}\right) \leq \kappa \zeta_i \epsilon \quad (41)$$

Substituting (36)-(38), (40), (41) into (35) yields

$$\begin{aligned} \dot{V}_2 \leq & -(k_1 - \frac{1}{2})\mathbf{e}_1^T \mathbf{e}_1 - (k_2 - \frac{1}{2})\mathbf{e}_2^T \mathbf{e}_2 \\ & -c_1(\mathbf{e}_1^T \mathbf{e}_1)^p - c_2(\mathbf{e}_2^T \mathbf{e}_2)^p + \frac{1}{2}\|\mathbf{l}_1\|^2 \\ & + \frac{1}{2}\|\mathbf{l}_2\|^2 + \sum_{i=1}^3 (\kappa \zeta_i \Xi + s_i n \\ & + \frac{n_1}{\gamma_i} \tilde{\zeta}_i \hat{\zeta}_i + \frac{s_i n_2}{\Gamma_i} \tilde{\beta}_i \hat{\beta}_i) \end{aligned} \quad (42)$$

According to the property of the square inequality, we have

$$\frac{n_1}{\gamma_i} \tilde{\zeta}_i \hat{\zeta}_i \leq -\frac{n_1}{2\gamma_i} \tilde{\zeta}_i^2 + \frac{n_1}{2\gamma_i} \zeta_i^2 \quad (43)$$

$$\frac{s_i n_2}{\Gamma_i} \tilde{\beta}_i \hat{\beta}_i \leq -\frac{s_i n_2}{2\Gamma_i} \tilde{\beta}_i^2 + \frac{s_i n_2}{2\Gamma_i} \beta_i^2 \quad (44)$$

Plugging (43) and (44) to (42) yields

$$\begin{aligned} \dot{V}_2 \leq & -(K_1 - \frac{1}{2})\mathbf{e}_1^T \mathbf{e}_1 - (K_2 - \frac{1}{2})\mathbf{e}_2^T \mathbf{e}_2 \\ & -c_1(\mathbf{e}_1^T \mathbf{e}_1)^p - c_2(\mathbf{e}_2^T \mathbf{e}_2)^p + \frac{1}{2}\|\mathbf{l}_1\|^2 + \frac{1}{2}\|\mathbf{l}_2\|^2 \\ & + \sum_{i=1}^3 (-n_1(\frac{\tilde{\zeta}_i^2}{2r_i})^p + n_1(\frac{\tilde{\zeta}_i^2}{2r_i})^p \\ & + s_i n_2(\frac{\tilde{\beta}_i^2}{2\Gamma_i})^p + s_i n_2(\frac{\tilde{\beta}_i^2}{2\Gamma_i})^p - \frac{n_1}{2r_i} \tilde{\zeta}_i^2 - \\ & \frac{s_i n_2}{2\Gamma_i} \tilde{\beta}_i^2 + s_i n + \kappa \zeta_i \Xi + \frac{n_1}{2\gamma_i} \zeta_i^2 + \frac{s_i n_2}{2\Gamma_i} \beta_i^2) \end{aligned} \quad (45)$$

For terms $n_1(\frac{\tilde{\zeta}_i^2}{2r_i})^p$ and $s_i n_2(\frac{\tilde{\beta}_i^2}{2\Gamma_i})^p$ in (45), the following conclusions are obtained from Lemma 2

$$n_1(\frac{\tilde{\zeta}_i^2}{2r_i})^p \leq \frac{n_1}{2\gamma_i} \tilde{\zeta}_i^2 + n_1(1-p)p^{\frac{1-p}{p}} \quad (46)$$

$$s_i n_2(\frac{\tilde{\beta}_i^2}{2\Gamma_i})^p \leq \frac{s_i n_2}{2\Gamma_i} \tilde{\beta}_i^2 + s_i n_2(1-p)p^{\frac{1-p}{p}} \quad (47)$$

Substituting (46) and (47) into (45) yields

$$\begin{aligned} \dot{V}_2 \leq & -(k_1 - \frac{1}{2})\mathbf{e}_1^T \mathbf{e}_1 - (k_2 - \frac{1}{2})\mathbf{e}_2^T \mathbf{e}_2 \\ & -\varkappa(\frac{1}{2}\mathbf{e}_1^T \mathbf{e}_1)^p - \varkappa(\frac{1}{2}\mathbf{e}_2^T \mathbf{e}_2)^p \\ & - \sum_{i=1}^3 (\varkappa(\frac{\tilde{\zeta}_i^2}{2\gamma_i})^p - \varkappa \frac{s_i n_2}{2\Gamma_i} (\tilde{\beta}_i^2)^p) + h \\ \leq & -\varrho V - \varkappa V^p + h \end{aligned} \quad (48)$$

where

$$\begin{aligned} \varrho = & \min\{k - \frac{1}{2}\}, \varkappa = \min\{2^p, c_1, c_2, n_1, s_i n_2\}, h = \\ & \frac{1}{2}\|\mathbf{l}_1\|^2 + \frac{1}{2}\|\mathbf{l}_2\|^2 + \sum_{i=1}^3 (s_i n + \kappa \zeta_i \Xi + \frac{n_1}{2\gamma_i} \zeta_i^2 + \frac{s_i n_2}{2\Gamma_i} \beta_i^2 + (n_1 + \\ & s_i n_2)(1-p)p^{\frac{1-p}{p}})(i=1, 2, 3). \end{aligned}$$

According to Lemma 3, the decrease of V_2 in finite time drives the tracking of the closed-loop system (1) into $V_2^p(e) \leq \frac{h}{(1-\lambda)\varkappa}$, and the trajectory is bounded in finite time as

$$\|e_i\| \leq \sqrt{2\left(\frac{h}{(1-\lambda)\varkappa}\right)^{1/p}} \quad (49)$$

The settling time satisfies

$$T \leq \frac{1}{\varkappa(1-p)} \ln \frac{\varkappa V^{1-p} + \lambda \varkappa}{\lambda \varkappa} \quad (50)$$

Obviously, ξ_1, ξ_2 can converge to zero in finite time, then (1) can achieve stability in finite time. Next, ξ_1, ξ_2 are proven bounded in finite time.

We construct a Lyapunov function

$$V_3 = \frac{1}{2}\xi_1^T \xi_1 + \frac{1}{2}\xi_2^T \xi_2 \quad (51)$$

The time derivative of V_3 is

$$\begin{aligned} \dot{V}_3 = & \xi_1^T (-k_1 \xi_1 + \mathbf{R}\bar{\alpha} - \mathbf{R}\alpha + \mathbf{R}\xi_2 - \mathbf{P}\mathbf{l}_1) \\ & + \frac{1}{2}\xi_2^T (-k_2 \xi_2 - \mathbf{R}\xi_1 - \mathbf{Q}\mathbf{l}_2) \\ = & -k_1 \xi_1^T \xi_1 - k_2 \xi_2^T \xi_2 + \xi_1^T \mathbf{R}(\bar{\alpha} - \alpha) \\ & - \sum_{i=1}^3 (l_{1i} |\xi_{1i}| - l_{2i} |\xi_{2i}|) \end{aligned} \quad (52)$$

According to [20], we can achieve

$$\|\mathbf{R}(\bar{\alpha} - \alpha)\| \leq \sum_{i=1}^3 \eta_i \quad (53)$$

where η_i is bounded.

At last, we have

$$\begin{aligned} \dot{V}_3 \leq & -k_1 \xi_1^T \xi_1 - k_2 \xi_2^T \xi_2 - \mathbf{l}_2 \xi_2 - \left(\sum_{i=1}^3 l_{1i} |\xi_{1i}| - \eta_i\right) \\ \leq & -d_1 V_3 - d_2 V_3^{\frac{1}{2}} \end{aligned} \quad (54)$$

where $d_1 = 2 \min\{k_1, k_2\}$ and $d_2 = \sqrt{2} \min\{l_{1i} - \eta_i\}$ are positive. According to [20], it is obtained that ξ_1, ξ_2 can converge to the origin in finite time. So, the tracking errors (10), (11) are practical finite stable. This completes the proof.

IV. NUMERICAL SIMULATIONS

We define the time interval $t=0.01s$, and a numerical simulation is conducted to verify the feasibility of our proposed method by using Matlab software.

A. Parameters Setting

In the numerical simulation, The structural parameters of the quadcopter UAV itself are: $m = 2.6\text{kg}$, $g = 9.8\text{N/s}^2$, $I_{xx} = 0.16\text{kg} \cdot \text{m}^2$, $I_{yy} = 0.16\text{kg} \cdot \text{m}^2$, $I_{zz} = 0.32\text{kg} \cdot \text{m}^2$, $k_u = 0.006\text{N} \cdot \text{m/s}$, $r_1 = 0.225\text{m}$, $r_2 = 0.25\text{m}$.

The controller-related parameters of the proposed scheme are chosen as $c_1 = 40$, $c_2 = 70$, $p = 0.99$, $\varpi = 8$, $n_1 = 20$, $n_2 = 16.8$, $\Gamma_i = \{1, 1, 1\}$, $\epsilon_i = \{10, 10, 10\}$, $r_i = \{10, 10, 10\}$, $\varepsilon = \text{diag}(20, 20, 20)$, $\mathbf{l}_1 = [0.1, 0.1, 0.1]^T$, $\mathbf{l}_2 = [0.15, 0.15, 0.15]^T$, $n = 8$, $k_1 = 20$, $k_2 = 10$.

B. Simulation experiments and analysis

The initial attitude values of the quadrotor UAV are given as $\Theta(0) = [-0.9, 0.9, 0.9]^T$, and the initial values of the filter is given $\xi_{1i}(0) = 0$, $\xi_{2i}(0) = 0$ and the initial values of ζ_i, β_i are given $\zeta_i(0) = 0$, $\beta_i(0) = 0$. The simulation time is set to 15s. The total lift given is equal to gravity, and simulate the attitude tracking effect of the quadrotor UAV in

hover state. In addition, in order to avoid the damage of the actuator mechanisms caused by the excessive output torques, the upper limit of each output control torque is restricted in the simulation process, and its maximum value does not exceed $0.18 \text{ N} \cdot \text{m}$.

In numerical simulations, the attitude curves are shown for the two cases of presence of actuator fault and absence of actuator fault respectively. Figure 2 shows the attitude tracking curves in the absence of actuator failure. It can be seen that the system output tracks the reference signal within 2.5 seconds. It is worth noting that the overshooting of this scenario is not significant. Fig. 3 shows the output curve under actuator failure. The system experiences an actuator fault at $t = 7.5 \text{ s}$ with a fault magnitude of $\rho = [0.6, 0.6, 0.6]^T$, $\sigma = [0.08, 0.08, 0.08]^T$. Despite the fact that the system experiences a severe actuator fault, the scheme still ensures that the system re-tracks the given reference signal within 1 s of the fault with a small steady state error.

Remark 2 According to Figures.3, it can be seen that the proposed scheme ensures that the quadrotor UAV tracks the reference signal for a limited period of time and has good handling capability for actuator faults. In addition, since a first-order low-pass filter is introduced, the problem of complex matrix computation is avoided, to ensure that the scheme is easy to implement. A compensation mechanism is introduced to further accelerate filtering error convergence times.

Figures 4 and 5 show the input signal curves in the two experiments, respectively, and it can be seen that the jitter vibration of the controller is not obvious, which also means that the scheme can be achieved in practical control. Figures 6 and 7 are the response curves of the filtering error. It is clear that e_{1i} and e_{2i} can converge to the equilibrium point within 3 seconds. Figures 8 and 9 represent the response curves of the adaptive law, and it can be seen that both β_i, ζ_i can converge near the equilibrium point.

V. CONCLUSIONS AND FUTURE WORK

In this paper, a finite-time control scheme is proposed for the attitude control system of quadrotor UAV. And a finite-time fault-tolerant control method is proposed based on the backstepping method and the command filtering technology. Differential explosion problem is solved. From the simulation results, the tracking effect is good, and the convergence speed is fast, and the steady-state error is small. However, the input saturation appears in the numerical simulation of the controller. In the future, a better control scheme will be used to solve this problem and further expand the application of other advanced theories and methods in UAV field.

REFERENCES

- [1] Robert van Steenberg, Martijn Mes, Wouter van Heeswijk, "Reinforcement learning for humanitarian relief distribution with trucks and UAVs under travel time uncertainty," *Transportation Research Part C: Emerging Technologies*, vol.157, pp.104401, 2023.
- [2] Yuan Gao, Ling Ren, Tianwei Shi, Teng Xu, and Jianbang Ding, "Autonomous Obstacle Avoidance Algorithm for Unmanned Aerial Vehicles Based on Deep Reinforcement Learning," *Engineering Letters*, vol.32, no.3, pp.650-660, 2024.
- [3] Li Yan, "Distributed optimization of heterogeneous UAV cluster PID controller based on machine learning", *Computers and Electrical Engineering*, vol.101, pp.108059, 2022.
- [4] Carlos A. Ramirez-Vanegas, and Eduardo Giraldo, "Real-time implementation of a Discrete Fractional-Order PID Control," *IAENG International Journal of Computer Science*, vol.48, no.1, pp.50-56, 2021.
- [5] Saleh Mobayen, "Adaptive fast-reaching nonsingular terminal sliding mode tracking control for quadrotor UAVs subject to model uncertainties and external disturbances", *Ain Shams Engineering Journal*, vol.14, pp.102059, 2023.
- [6] Karim Ahmadi, Davood Asadi, Abdelrazzak Merheb,"Active fault-tolerant control of quadrotor UAVs with nonlinear observer-based sliding mode control validated through hardware in the loop experiments", *Control Engineering Practice*, vol.137, pp.105557, 2023.
- [7] Moussa Labbadi, Yassine Boukal, Mohamed Cherkaoui, Mohamed Djemai, Fractional-order global sliding mode controller for an uncertain quadrotor UAVs subjected to external disturbances, *Journal of the Franklin Institute*, vol.358, pp.4822-4847, 2021.
- [8] Guoyuan Qi, Jiahao Deng, Xia Li, Xinchun Yu, Compensation function observer-based model-compensation backstepping control and application in anti-inference of quadrotor UAV, *Control Engineering Practice*, vol.140, Pages 105633, 2023.
- [9] Yakoub Nettari, Moussa Labbadi, Serkan Kurt, "Adaptive Backstepping Integral Sliding Mode Control Combined with Super-Twisting Algorithm For Nonlinear UAV Quadrotor System", *IFAC-Papers OnLine*, vol.55, pp.264-269, 2022.
- [10] Ning Wang, Chunjiang Qian, Jing-Chao Sun, "Adaptive robust finite-time trajectory tracking control of fully actuated marine surface vehicles", *IEEE Trans. on Control Systems Technology*, vol.24, no.4, pp.1454-1462, 2016.
- [11] Yakoub Nettari, Serkan Kurt, Moussa Labbadi, "Adaptive Robust Control based on Backstepping Sliding Mode techniques for Quadrotor UAV under external disturbances", *IFAC-PapersOnLine*, vol.55 pp.252-257, 2022.
- [12] Shogo Hirano, Kenji Uchiyama, Kai Masuda,"Controller Design Using Backstepping Algorithm for Fixed-Wing UAV with Thrust Vectoring System", 2019 International Conference on Unmanned Aircraft Systems (ICUAS), pp.1084-1088, 2019.
- [13] Kang Liu, Rujing Wang, Xiaodong Wang, Xingxian Wang, "Anti-saturation adaptive finite-time neural network based fault-tolerant tracking control for a quadrotor UAV with external disturbances", *Aerospace Science and Technology*, vol.115, pp.106790, 2021.
- [14] Yujiang Zhong, Youmin Zhang, Wei Zhang, Junyi Zuo, "Robust Actuator Fault Detection and Diagnosis for a Quadrotor UAV With External Disturbances", in *IEEE Access*, vol.6, pp.48169-48180, 2018.
- [15] Thanaraj T., Kin Huat Low, Bing Feng Ng, "Actuator fault detection and isolation on multi-rotor UAV using extreme learning neuro-fuzzy systems", *ISA Transactions*, vol.138, pp.168-185,2023
- [16] Ziquan Yu, Youmin Zhang, Bin Jiang, Chun-Yi Su, Jun Fu, Ying Jin, Tianyou Chai,"Nussbaum-based finite-time fractional-order backstepping fault-tolerant flight control of fixed-wing UAV against input saturation with hardware-in-the-loop validation,"*Mechanical Systems and Signal Processing*, vol.153 pp.107406, 2021.
- [17] Omid Mofid, Saleh Mobayen,"Adaptive sliding mode control for finite-time stability of quad-rotor UAVs with parametric uncertainties" *ISA Transactions*, vol.72, pp.1-14, 2018.
- [18] Yaobang Zang, Xinyu Ouyang, Nannan Zhao, and Jiangnan Zhao, "Event-triggered Finite-time Prescribed Performance Output-feedback Control for Nonlinear Systems with Unmodeled Dynamics," *Engineering Letters*, vol.32, no.4, pp.743-752, 2024.
- [19] Yakoub Nettari, Moussa Labbadi, Serkan Kurt, "Adaptive robust finite time tracking control for quadrotor subject to disturbances", *Advances in Space Research*, vol.71, pp.3803-3821, 2023.
- [20] Yuan-Xin Li, "Finite time command filtered adaptive fault tolerant control for a class of uncertain nonlinear systems", *Automatica*, vol.106, pp.117-123, 2019.
- [21] M. M. Polycarpou, "Stable adaptive neural control scheme for nonlinear systems", *IEEE Transactions on Automatic Control*, vol.41, no.3, pp.447-451, 1996.
- [22] Hui Wang, Quanxin Zhu, "Adaptive output feedback control of stochastic nonholonomic systems with nonlinear parameterization", *Automatica*, vol.98, pp.247-255, 2018.
- [23] Jitu Sanwale, Suresh Dahiya, Prasiddh Trivedi, Mangal Kothari, Robust fault-tolerant adaptive integral dynamic s liding mode control using finite-time disturbance observer for coaxial octorotor UAVs, *Control Engineering Practice*, vol.135, pp.105495, 2023.
- [24] Karam Elikar, Weidong Zhang, "Finite-time adaptive integral backstepping fast ter minal sliding mode control application on quadrotor UAV", *International Journal of Control, Automation and Systems*, vol.18, pp.415-430, 2020.
- [25] Wenqian Liu, Xianghong Cheng, Jingjing Zhang, "Command filter-based adaptive fuzzy integral backstepping control for quadrotor UAV with input saturation", *Journal of the Franklin Institute*, vol.360, pp.484-507, 2023.

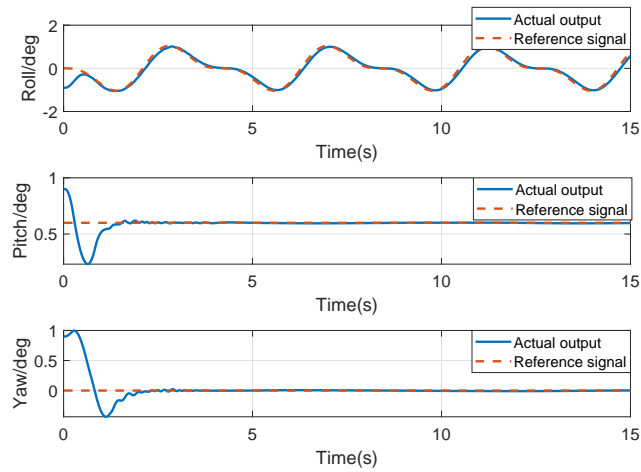


Fig. 2. Output tracking response curves of the UAV without failures.

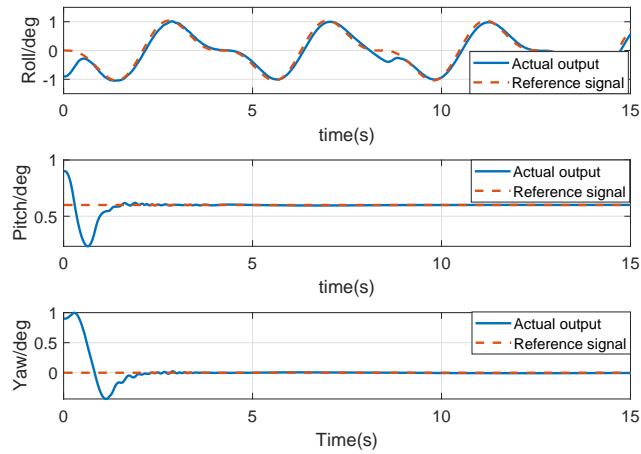


Fig. 3. Output tracking response curves of the UAV with failures.

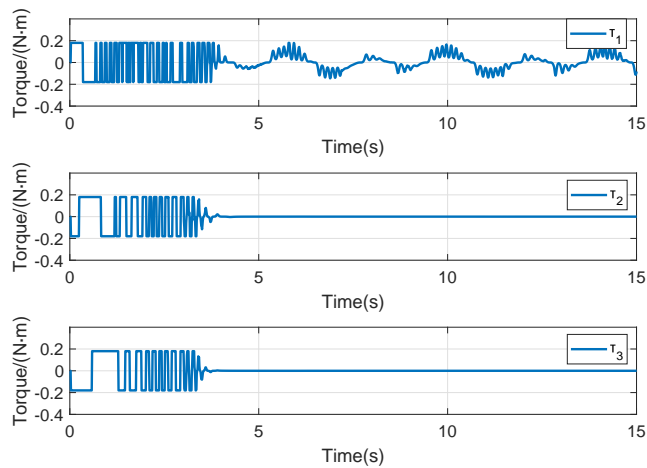


Fig. 4. Control torque response curves of fault-free case.

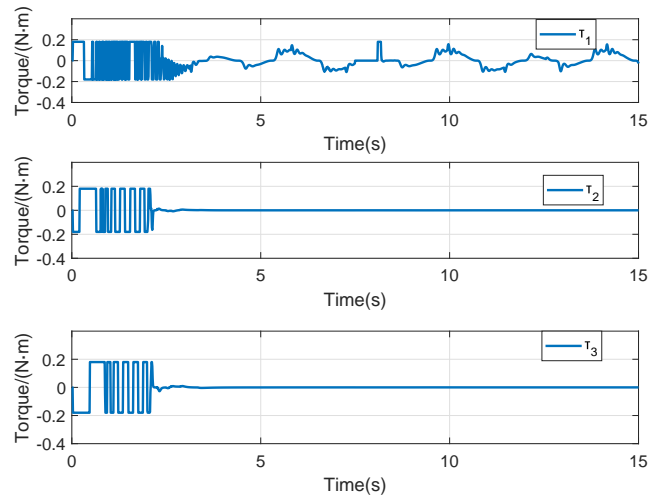


Fig. 5. Control torque response curves of partial fault.

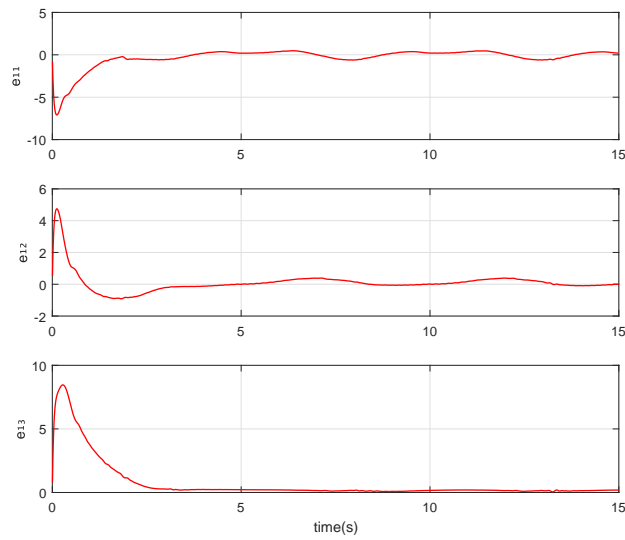


Fig. 6. Response curves of e_{1i} .

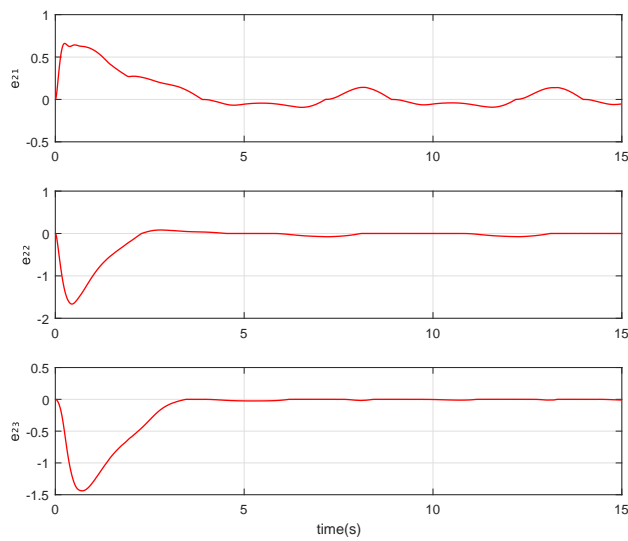


Fig. 7. Response curves of e_{2i} .

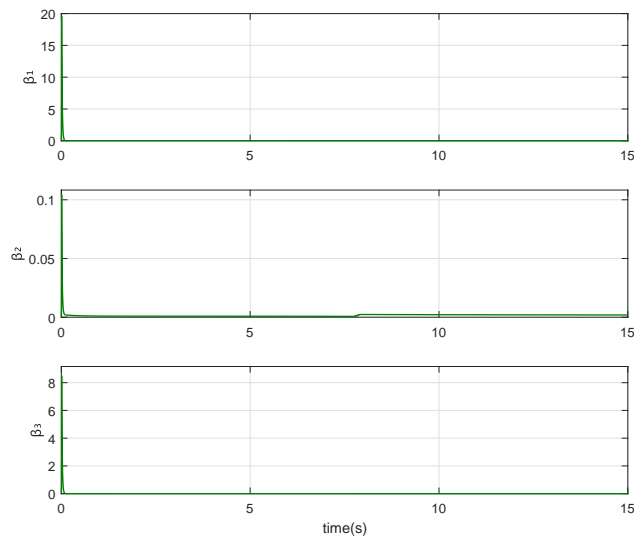


Fig. 8. Response curves of β_i .

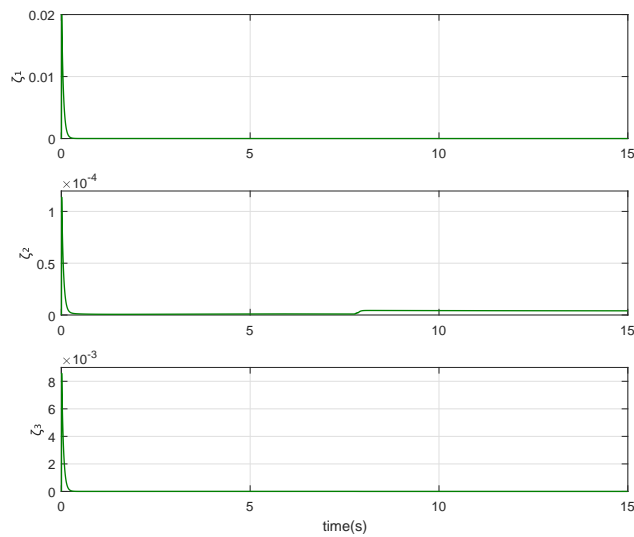


Fig. 9. Response curves of ζ_i .